the FEBS Journal

A carboxylated Zn-phthalocyanine inhibits fibril formation of Alzheimer's amyloid β peptide

Shatera Tabassum[1], Abdullah M. Sheikh[1], Shozo Yano[1], Takafumi Ikeue[2], Makoto Handa[2] and Atsushi Nagai[1]

1 Department of Laboratory Medicine, Shimane University School of Medicine, Izumo, Japan
2 Department of Material Science, Interdisciplinary Faculty of Science and Engineering, Shimane University, Matsue, Japan

Keywords
Alzheimer's disease; amyloid β peptide; fibril formation; near infrared; phthalocyanine

Correspondence
A. Nagai, Department of Laboratory Medicine, Shimane University School of Medicine, 89-1 Enya Cho, Izumo 693-8501, Japan
Fax: +81 853 20 2312
Tel: +81 853 20 2312
E-mail: anagai@med.shimane-u.ac.jp

(Received 27 May 2014, revised 7 November 2014, accepted 14 November 2014)

doi:10.1111/febs.13151

Amyloid β (Aβ), a 39–42 amino acid peptide derived from amyloid precursor protein, is deposited as fibrils in Alzheimer's disease brains, and is considered to play a major role in the pathogenesis of the disease. We have investigated the effects of a water-soluble Zn-phthalocyanine, ZnPc $(COONa)_8$, a macrocyclic compound with near-infrared optical properties, on Aβ fibril formation *in vitro*. A thioflavin T fluorescence assay showed that ZnPc$(COONa)_8$ significantly inhibited Aβ fibril formation, increasing the lag time and dose-dependently decreasing the plateau level of fibril formation. Moreover, it destabilized pre-formed Aβ fibrils, resulting in an increase in low-molecular-weight species. After fibril formation in the presence of ZnPc$(COONa)_8$, immunoprecipitation of $Aβ_{1-42}$ using Aβ-specific antibody followed by near-infrared scanning demonstrated binding of ZnPc$(COONa)_8$ to $Aβ_{1-42}$. A study using the hydrophobic fluorescent probe 8-anilino-1-naphthalenesulfonic acid showed that ZnPc$(COONa)_8$ decreased the hydrophobicity during $Aβ_{1-42}$ fibril formation. CD spectroscopy showed an increase in the α helix structure and a decrease in the β sheet structure of $Aβ_{1-40}$ in fibril-forming buffer containing ZnPc $(COONa)_8$. SDS/PAGE and a dot-blot immunoassay showed that ZnPc $(COONa)_8$ delayed the disappearance of low-molecular-weight species and the appearance of higher-molecular-weight oligomeric species of $Aβ_{1-42}$. A cell viability assay showed that ZnPc$(COONa)_8$ was not toxic to a neuronal cell line (A1), but instead protected A1 cells against $Aβ_{1-42}$-induced toxicity. Overall, our results indicate that ZnPc$(COONa)_8$ binds to Aβ and decreases the hydrophobicity, and this change is unfavorable for Aβ oligomerization and fibril formation.

Introduction

Alzheimer's disease (AD) is a common dementia of the elderly [1]. It is characterized pathologically by degeneration of neurons, mainly of the cholinergic type, in the hippocampal and cortical areas [2,3]. Histologically, dystrophic neurons and reactive glial cells are found in these areas, concomitant with extracellular deposition of amyloid β (Aβ) peptide and intracellular formation of neurofibrillary tangles [2]. A large body of evidence suggests that Aβ peptide has a critical role in the pathogenesis of AD. For example, gene mutations that affect the production or processing of Aβ precursor protein and increase the peptide burden, are

Abbreviations
Aβ, amyloid β peptide; AD, Alzheimer's disease; ANS, 8-anilino-1-naphthalenesulfonic acid; MTT, 3-(4,5-dimethylthiazol-2-yl)-2, 5-diphenyltetrazolium bromide; ThT, thioflavin T; ZnPc, Zn-containing phthalocyanine.

related to AD lesion formation and progression of the disease [4–10]. An increased Aβ peptide burden leads to aggregation, producing oligomers or polymeric fibrils that are deposited in the brain parenchyma [6]. Aggregated forms, especially Aβ oligomers, are more neurotoxic than the monomers *in vitro* [11,12], suggesting that Aβ accumulation and aggregation play key roles in disease pathogenesis. Hence, these processes may be good targets for diagnosis and treatment of AD.

Recent research on the pathophysiology of AD has suggested that inhibitors of Aβ accumulation and aggregation, or enhancers of fibril degradation, are candidates for treatment of the disease [13,14]. Several compounds that have shown anti-amyloid activity *in vitro* or in animal models are already in clinical trials [13,14]. However, an effective disease-modifying treatment remains elusive.

Diagnosis is also an important issue, and several groups are examining the usefulness of Aβ peptide in cerebrospinal fluid or deposited in brain parenchyma as a diagnostic marker [15,16]. Deposited Aβ may be visualized by positron emission tomography (PET) imaging, but the equipment is expensive and not widely available [16]. In contrast, near-infrared (NIR) spectroscopy is technically favorable for *in vivo* imaging, because there is an optical window from approximately 600 to 1000 nm, at which the absorption coefficient of the tissue is at a minimum, resulting in a low background [17]. NIR light has higher tissue-penetration capability than visible light [17]. Recently, it was reported that phthalocyanines, which are metal-containing, aromatic, macrocyclic NIR fluorophores, interact with α-synuclein and affect fibril formation [18]. Further, iron-containing phthalocyanine interacts with toxic $A\beta_{1\text{-}40}$ oligomers and converts them to an amyloid fibril meshwork [19]. Thus, we hypothesized that phthalocyanines may bind to Aβ and serve as amyloid fibril-modifying agents. If this is the case, they may have therapeutic potential for AD. They may also be useful as amyloid-specific NIR imaging probes to visualize deposited Aβ peptide in AD brains *in vivo*.

Most phthalocyanine species are hydrophobic, and tend to aggregate in aqueous medium, resulting a self-quenching effect on their excited state [20,21]. Therefore, we prepared water-soluble Zn-containing phthalocyanines (ZnPcs) bearing sodium carboxylate groups as candidate amyloid fibril-modifying agents or *in vivo* NIR probes. The chemical structures of the four phthalocyanines used in this study are shown in Fig. 1. Among them, carboxylated ZnPcs were found to bind with Aβ peptide and to inhibit Aβ aggregation and neurotoxicity.

Results

Interactions of phthalocyanines with $A\beta_{1\text{-}40}$ and $A\beta_{1\text{-}42}$ and effect on fibril formation

$A\beta_{1\text{-}42}$ (12.5 μM) and $A\beta_{1\text{-}40}$ (50 μM) were incubated for 24 or 48 h, respectively, with increasing concentrations of $ZnPc(COONa)_8$, $ZnPc(COONa)_{16}$, $ZnPc(COOC_5H_{11})_8$ and Pd-containing phthalocyanine (PdPc) dimer in fibril-forming buffer. Evaluation of fibril formation by a thioflavin T (ThT) fluorescence assay revealed that $ZnPc(COONa)_8$ efficiently and dose-dependently inhibited fibril formation for both $A\beta_{1\text{-}40}$ and $A\beta_{1\text{-}42}$ (Fig. 2A,B). The effect was more pronounced in the case of $A\beta_{1\text{-}40}$ (compare Fig. 2A and Fig. 2B). $ZnPc(COONa)_{16}$ also modestly inhibited $A\beta_{1\text{-}40}$ and $A\beta_{1\text{-}42}$ fibril formation at higher concentrations (Fig. 2C,D). The PdPc dimer inhibited only $A\beta_{1\text{-}40}$ fibril formation at relatively high concentrations (Fig. 2G,H). On the other hand, $ZnPc(COOC_5H_{11})_8$ significantly and dose-dependently increased fibril formation of $A\beta_{1\text{-}40}$, but not that of $A\beta_{1\text{-}42}$ (Fig. 2E,F).

Effects of $ZnPc(COONa)_8$ on fibril formation kinetics of $A\beta_{1\text{-}40}$ and $A\beta_{1\text{-}42}$

In order to investigate the fibril formation kinetics, $A\beta_{1\text{-}40}$ (50 μM) or $A\beta_{1\text{-}42}$ (12.5 μM) were incubated in the absence or presence of 5 μM $ZnPc(COONa)_8$. Fibril formation for both $A\beta_{1\text{-}40}$ and $A\beta_{1\text{-}42}$ showed sigmoid kinetics, with lag times of approximately 12 and 8 h, respectively (Fig. 3A,B). Once fibril formation started, it increased exponentially, reaching a plateau at 48 h for $A\beta_{1\text{-}40}$ and 24 h for $A\beta_{1\text{-}42}$ (Fig. 3A,B). The presence of $ZnPc(COONa)_8$ extended the lag time to 24 h and the plateau time to 72 h for $A\beta_{1\text{-}40}$ (Fig. 3C). For $A\beta_{1\text{-}42}$, the lag time was slightly increased to between 8 and 16 h, while the plateau time showed little change (Fig. 3D). $ZnPc(COONa)_8$ significantly decreased the plateau fluorescence levels of both $A\beta_{1\text{-}40}$ (57 ± 8.3 for $A\beta_{1\text{-}40}$ versus 12.3 ± 2.4 for $A\beta_{1\text{-}40}$ + $ZnPc(COONa)_8$) and $A\beta_{1\text{-}42}$ (20.1 ± 0.8 for $A\beta_{1\text{-}42}$ versus 4.5 ± 0.4 for $A\beta_{1\text{-}42}$ + $ZnPc(COONa)_8$). The morphology of the Aβ fibrils was evaluated by transmission electron microscopy. $ZnPc(COONa)_8$ had no apparent effect on the morphology of $A\beta_{1\text{-}40}$ or $A\beta_{1\text{-}42}$ fibrils (Fig. 3E).

In this study, ThT fluorescence assay was mainly employed for quantitative analysis of Aβ fibrils. However, the presence of $ZnPc(COONa)_8$ may influence ThT fluorescence [22]. Therefore, to confirm the inhibitory effect, fibrils were removed from the samples by filtration after fibril formation for $A\beta_{1\text{-}42}$ (100 μM) in

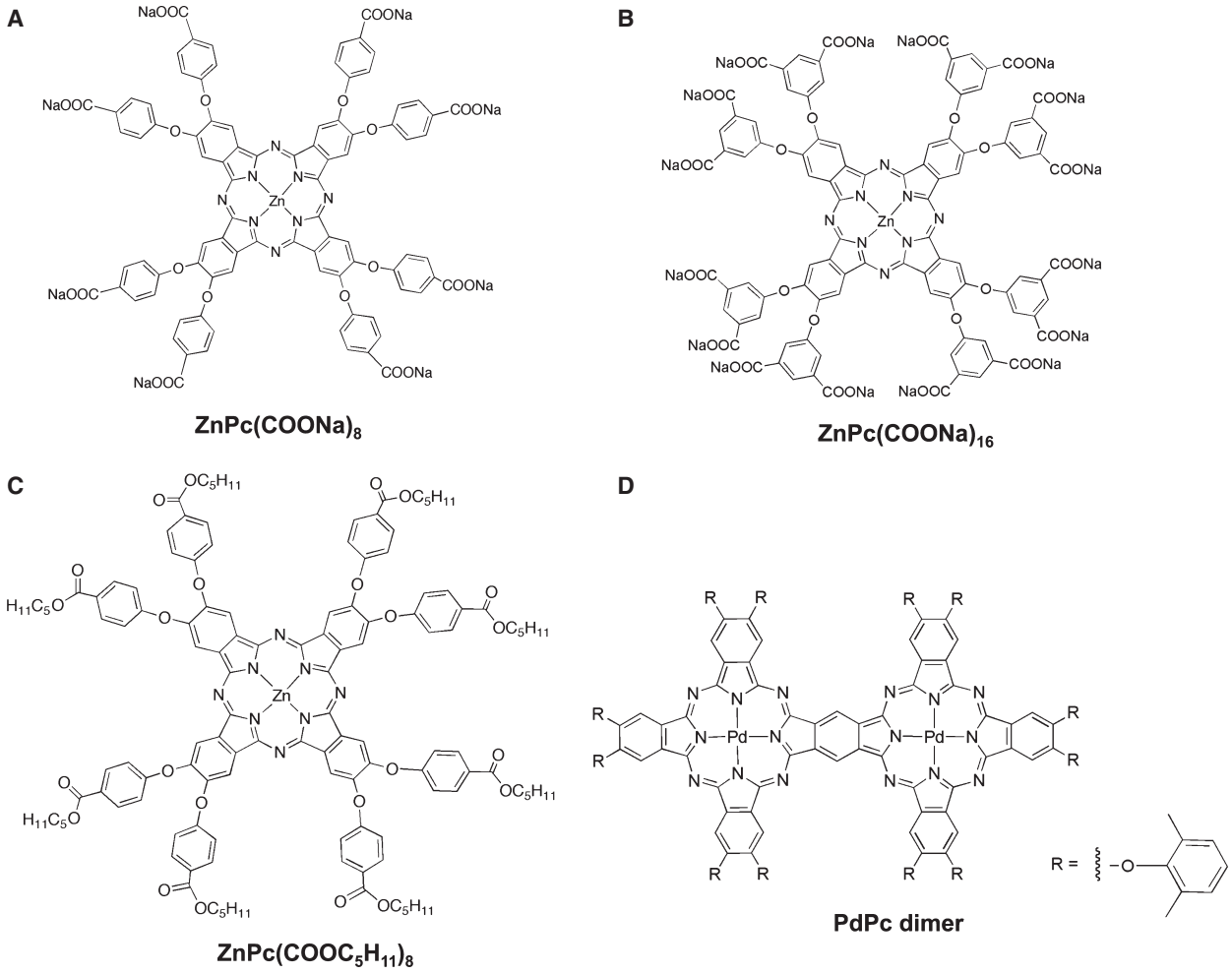

Fig. 1. Chemical structures of $ZnPc(COONa)_8$ (A), $ZnPc(COONa)_{16}$ (B), $ZnPc(COOC_5H_{11})_8$ (C) and the PdPc dimer (D).

the absence or presence of $ZnPc(COONa)_8$ (5 μM) for 24 h. The filtrate contained only non-fibrillar $A\beta_{1\text{-}42}$, as revealed by the ThT fluorescence assay. The protein concentration of the filtrate was measured, and was 235 ± 8.2% higher in the $A\beta_{1\text{-}42}$ sample containing $ZnPc(COONa)_8$ compared to $A\beta_{1\text{-}42}$ alone (Fig. 3F). This result supports the view that $ZnPc(COONa)_8$ inhibits fibril formation.

Effect of $ZnPc(COONa)_8$ on the stability of Aβ fibrils

Next, the effect of $ZnPc(COONa)_8$ on the stability of Aβ fibrils was investigated. Increasing concentrations of $ZnPc(COONa)_8$ were added to pre-formed $A\beta_{1\text{-}40}$ and $A\beta_{1\text{-}42}$ fibrils, and the mixtures were incubated for 24 h. The ThT fluorescence assay showed that $ZnPc(COONa)_8$ dose-dependently decreased both $A\beta_{1\text{-}40}$ and $A\beta_{1\text{-}42}$ fibril levels at the end of the incubation period (Fig. 4A,B). Moreover, SDS/PAGE confirmed that $ZnPc(COONa)_8$ increased the levels of low-molecular-weight species of $A\beta_{1\text{-}40}$ and $A\beta_{1\text{-}42}$, at least at high concentrations (Fig. 4C,D).

Effects of sodium azide on Aβ fibril formation

Phthalocyanines are reported to produce singlet oxygen [23]. Therefore, we investigated whether singlet oxygen is responsible for the inhibitory effect of $ZnPc(COONa)_8$ by using sodium azide (NaN_3) as a scavenger of singlet oxygen [24]. We first confirmed that NaN_3 alone (up to 50 mM) had no effect on $A\beta_{1\text{-}40}$ and $A\beta_{1\text{-}42}$ fibril formation (Fig. 5A,B). Next, $A\beta_{1\text{-}40}$ and $A\beta_{1\text{-}42}$ were incubated with increasing concentrations of NaN_3 (up to 50 mM) in the presence of $ZnPc(COONa)_8$. The ThT fluorescence assay indicated that NaN_3 had no effect on $ZnPc(COONa)_8$-mediated inhibition of $A\beta_{1\text{-}40}$ and $A\beta_{1\text{-}42}$ fibril formation (Fig. 5C,D).

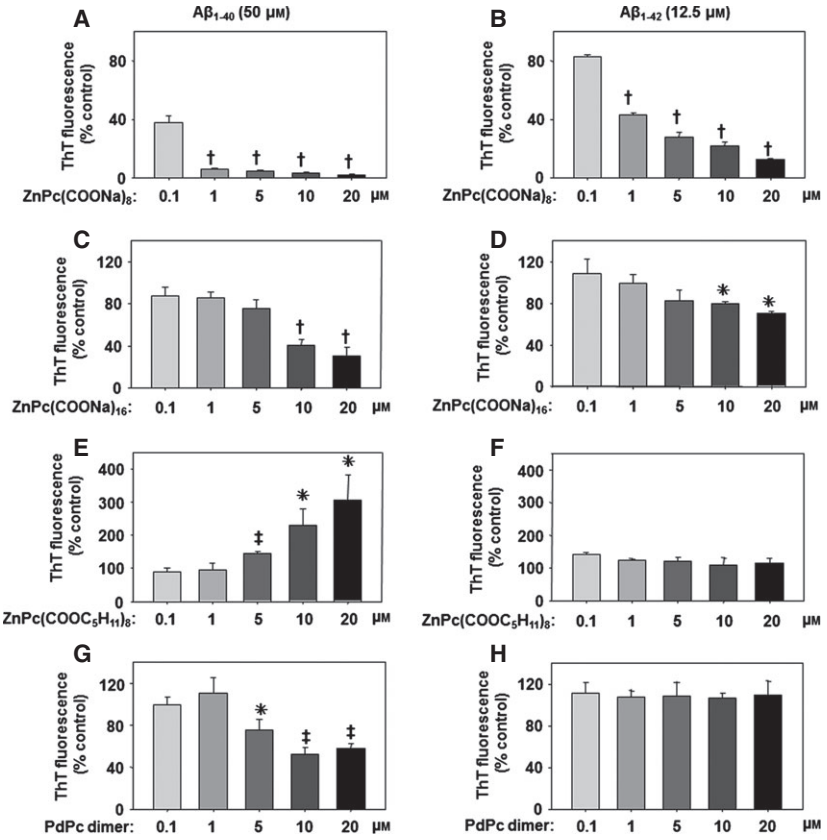

Fig. 2. Effect of phthalocyanines on Aβ peptide fibril formation. $A\beta_{1\text{-}40}$ peptide (50 μM) (A,C,E,G) or $A\beta_{1\text{-}42}$ peptide (12.5 μM) (B,D,F,H) were incubated in fibril-forming buffer for 48 and 24 h, respectively, in the presence of the indicated concentrations of $ZnPc(COONa)_8$ (A,B), $ZnPc(COONa)_{16}$ (C,D), $ZnPc(COOC_5H_{11})_8$ (E,F) or PdPc dimer (G,H). Total fibril formation at the end of incubation was evaluated by the ThT fluorescence assay, as described in Experimental procedures. Values are means ± SEM of at least three independent experiments, and are presented as a percentage of the control condition (Aβ peptide alone). Symbols indicate statistically significant differences compared with the corresponding 0.1 μM phthalocyanine condition (*$P < 0.05$, ‡$P < 0.01$, †$P < 0.001$).

Binding of $ZnPc(COONa)_8$ to $A\beta_{1\text{-}42}$ peptide

We investigated whether $ZnPc(COONa)_8$ directly binds to Aβ peptide by adding increasing concentrations of $ZnPc(COONa)_8$ to $A\beta_{1\text{-}42}$ monomers or pre-formed fibrils. After incubation for 24 h in a fibril-forming environment, $A\beta_{1\text{-}42}$ was immunoprecipitated using Aβ-specific antibody, and the amount of $ZnPc(COONa)_8$ in the immunoprecipitate was quantified by NIR scanning. In the case of the $A\beta_{1\text{-}42}$ monomer, the NIR signal of $ZnPc(COONa)_8$ in the immunoprecipitates increased linearly with increasing concentration of the compound (Fig. 6A). A similar effect was observed with pre-formed $A\beta_{1\text{-}42}$ fibrils, although the signal intensities were much lower than with the $A\beta_{1\text{-}42}$ monomer (Fig. 6A).

Effect of ZnPc on the microenvironment of fibril formation

To further explore the mechanism of inhibition, we investigated whether binding of $ZnPc(COONa)_8$ alters the microenvironment of Aβ fibril formation. Hydrophobic amino acids in the Aβ peptide, as well as a hydrophobic microenvironment, play a key role in fibril formation [25–27]. We used 8-anilino-1-naphthalenesulfonic acid (ANS) as a hydrophobic fluorescent probe; its fluorescence in aqueous solution is minimal, but, upon binding to non-polar amino acids, the fluorescence increases and shows a blue shift [28]. Hence, ANS is useful to analyze conformational changes of proteins or peptides in solution. We found that incubation of $A\beta_{1\text{-}42}$ in fibril-forming buffer for 4 h caused an increase in the fluorescence intensity, together with a blue shift (Fig. 6B–D). However, when $ZnPc(COONa)_8$ was added to the buffer, the intensity decreased significantly, and the peak showed a red shift compared to $A\beta_{1\text{-}42}$ only (Fig. 6B–D).

Effect of $ZnPc(COONa)_8$ on the secondary structures and molecular species of Aβ peptide

Hydrophobic interactions are important in secondary structure formation and aggregation of Aβ peptides [25,29,30]. As $ZnPc(COONa)_8$ decreased the hydrophobicity of Aβ, we investigated whether it influenced the secondary structures of the peptide. $ZnPc(COONa)_8$ (2 μM) was added to $A\beta_{1\text{-}40}$ (100 μM) monomer in a fibril-forming buffer, and the mixture was incubated at 37°C for 0 and 2 h, then diluted with water to final concentrations of $A\beta_{1\text{-}40}$ and $ZnPc(COONa)_8$ of 10 and 0.2 μM, respectively. Representative CD

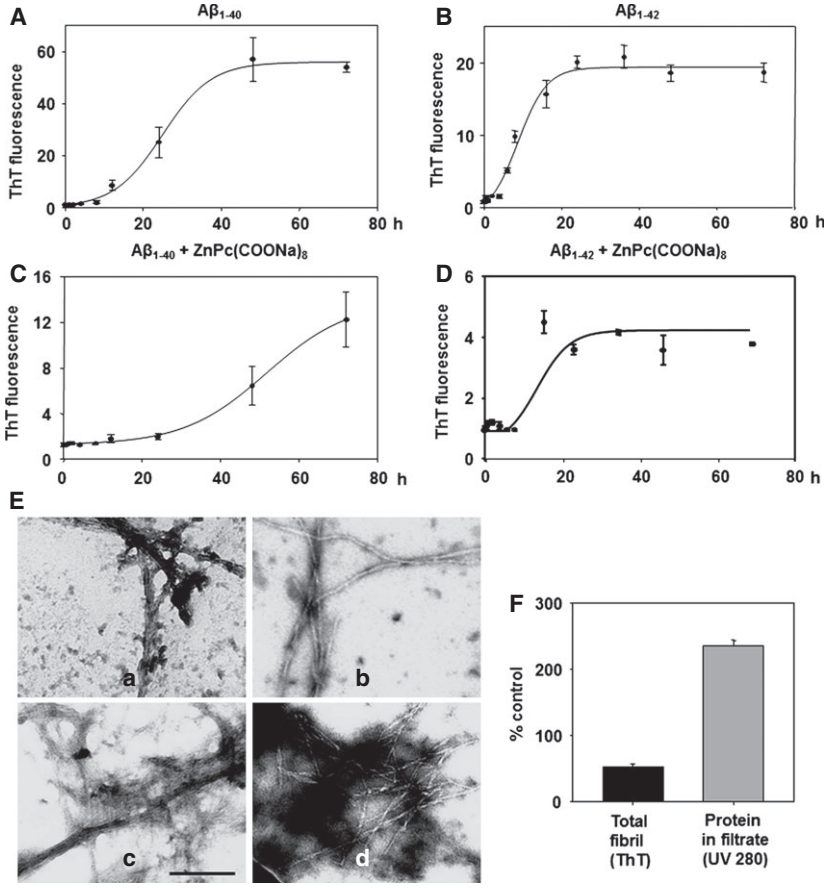

Fig. 3. Effects of $ZnPc(COONa)_8$ on the fibril formation kinetics of Aβ peptides. (A–D) $A\beta_{1-40}$ peptide (50 μM) (A,C) or $A\beta_{1-42}$ peptide (12.5 μM) (B,D) were incubated in fibril-forming buffer in the absence (A,B) or presence (C,D) of $ZnPc(COONa)_8$ (5 μM) for the indicated times. Total fibril formation at the end of incubation was evaluated by ThT fluorescence assay, as described in Experimental procedures. Values are means ± SEM of ThT fluorescence values (arbitrary units) for at least three independent experiments. (E) The morphology of Aβ fibrils. $A\beta_{1-40}$ peptides (a,c) and $A\beta_{1-42}$ peptides (b,d) (50 μM) were incubated in the absence (a,b) or presence (c,d) of $ZnPc(COONa)_8$ (5 μM) for 72 and 24 h, respectively. Fibril morphology was evaluated by transmission electron microscopy as described in Experimental procedures. Scale bar = 200 nm. (F) $A\beta_{1-42}$ peptide (100 μM) was incubated alone or with $ZnPc(COONa)_8$ (5 μM) for 24 h. Aliquots of the samples were used for the ThT fluorescence assay (left bar). From the remaining samples, fibrils were removed by filtration, and protein in the filtrates (right bar) was measured using a UV/Vis spectrophotometer at 280 nm, as described in Experimental procedures. Values are means ± SEM of three independent experiments, and are expressed as a percentage of the control condition ($A\beta_{1-42}$ peptide alone).

spectra of $A\beta_{1-40}$ in the presence or absence of $ZnPc(COONa)_8$ after 0 and 2 h incubation are shown in Fig. 7A. The CD spectroscopy experiments (Fig. 7B) indicated that, in fibril formation buffer, approximately 37.2 ± 7.6% of the peptide adopted a β sheet structure, whereas only 5 ± 2.3% showed an α helix structure. After 2 h incubation, the percentage of α helix showed little change (3.7 ± 1.5%), but the proportion of β sheet increased to 48.6 ± 0.2%. When $ZnPc(COONa)_8$ was added to the fibril-forming buffer, 18.7 ± 0.9% of the peptide exhibited α helix structure, and 4.9 ± 3% adopted β sheet. After 2 h incubation, the percentages of α helix and β sheet were 17.6 ± 3.5 and 17.2 ± 5.9, respectively.

After fibril formation in the absence or presence of $ZnPc(COONa)_8$, the peptide was subjected to SDS/PAGE, and Aβ species were visualized by Coomassie Blue staining. $A\beta_{1-42}$ was detected mainly as monomers, dimers and trimers. Dimers and trimers started to decrease after 1 h incubation, and monomers decreased from 2 h. $ZnPc(COONa)_8$ inhibited the time-dependent decrease in these low-molecular-weight $A\beta_{1-42}$ species at 1, 2 and 4 h (Fig. 7C).

Then, the effect of $ZnPc(COONa)_8$ on $A\beta_{1-42}$ oligomers was investigated. A dot-blot immunoassay using an oligomer-specific antibody demonstrated that $A\beta_{1-42}$ oligomers were detectable after 4 h incubation (Fig. 7D). $ZnPc(COONa)_8$ delayed $A\beta_{1-42}$

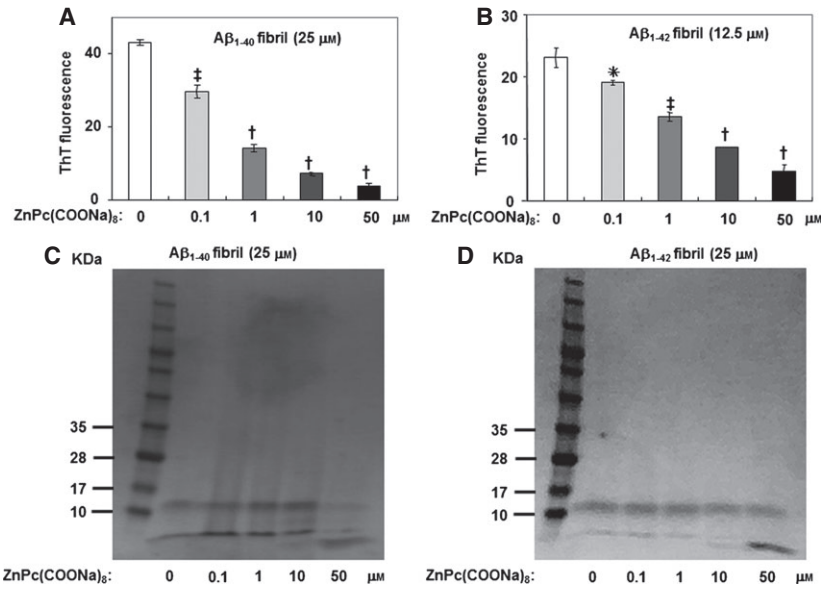

Fig. 4. Effect of ZnPc(COONa)$_8$ on Aβ fibril stability. To prepare fibrils, Aβ$_{1\text{-}40}$ peptide (50 μM) and Aβ$_{1\text{-}42}$ peptide (25 μM) were incubated in fibril-forming buffer for 48 and 24 h, respectively. The indicated concentrations of ZnPc(COONa)$_8$ were added (final concentrations of peptide 25 and 12.5 μM, respectively), and incubation was continued for 24 h. (A,B) Total fibrils of Aβ$_{1\text{-}40}$ (A) and Aβ$_{1\text{-}42}$ (B) were evaluated by a ThT fluorescence assay. Values are means ± SEM of ThT fluorescence values (arbitrary unit) for at least three experiments. (C,D) Aβ$_{1\text{-}40}$ or Aβ$_{1\text{-}42}$ were incubated in fibril-forming buffer for 48 and 24 h, respectively. Then the indicated concentrations of ZnPc(COONa)$_8$ were added (final concentration of peptide 25 μM) and incubation was continued for 24 h. Two micrograms of peptide fibrils were separated by SDS/PAGE using a 4-20% gradient Tris-glycine gel, and the peptide bands for Aβ$_{1\text{-}40}$ (C) and Aβ$_{1\text{-}42}$ (D) were visualized by Coomassie Brilliant Blue staining, as described in Experimental procedures. Symbols indicate statistically significant differences compared with the corresponding 0 μM ZnPc(COONa)$_8$ condition ($^*P < 0.05$, $^‡P < 0.01$, $^†P < 0.001$).

oligomers formation, which was detectable from 8 h (Fig. 7D).

Effect of ZnPc(COONa)$_8$ on Aβ$_{1\text{-}42}$-induced cytotoxicity

Oligomers of Aβ peptides are considered to be more cytotoxic than monomers [11,12]. As ZnPc(COONa)$_8$ inhibited oligomer formation, we explored whether it affected Aβ$_{1\text{-}42}$-induced cytotoxicity in a neuronal cell line (A1). Morphological study of cultured A1 cells showed that increasing concentrations of Aβ$_{1\text{-}42}$ decreased the cell density, and the cell body became round and smaller in size (Fig. 8A). ZnPc(COONa)$_8$ alone did not alter the density or morphology of the cultured cells (Fig. 8A). Interestingly, addition of ZnPc(COONa)$_8$ to the culture partially recovered the cells from Aβ$_{1\text{-}42}$-induced reduction of cell density and morphological change (Fig. 8B).

To further examine the cytotoxic properties, cell viability was evaluated by an 3-(4,5-dimethylthiazol-2-yl)-2,5-diphenyltetrazolium bromide (MTT) assay. A1 cells were cultured in the presence of increasing concentrations of Aβ$_{1\text{-}42}$ or ZnPc(COONa)$_8$ for 48 h, and the MTT assay was performed. Aβ$_{1\text{-}42}$ dose-dependently decreased the viability of A1 cells, whereas ZnPc(COONa)$_8$ did not (Fig. 8C). However, when A1 cells were cultured with 5 μM Aβ$_{1\text{-}42}$, ZnPc (COONa)$_8$ partially rescued the cells from Aβ$_{1\text{-}42}$-induced cytotoxicity in a dose-dependent manner (Fig. 8D).

Discussion

The present results indicate that a water-soluble Zn-phthalocyanine, ZnPc(COONa)$_8$, binds to Aβ peptide and inhibits aggregation, apparently by altering the microenvironment for fibril formation. This is important, because Aβ aggregation and deposition play a vital role in the pathogenesis of AD, and may be useful as a disease marker [2]. As ZnPc(COONa)$_8$ shows NIR optical properties, it may have potential as a diagnostic imaging probe for AD, in addition to being a candidate therapeutic agent.

The inhibitory effects on Aβ fibril formation were both dose-dependent and dependent on the species of phthalocyanine. It has been reported that tetrasulfonated phthalocyanines interact with α-synuclein during the fibril formation process in a manner that depends on the nature of the metal at the macrocyclic center

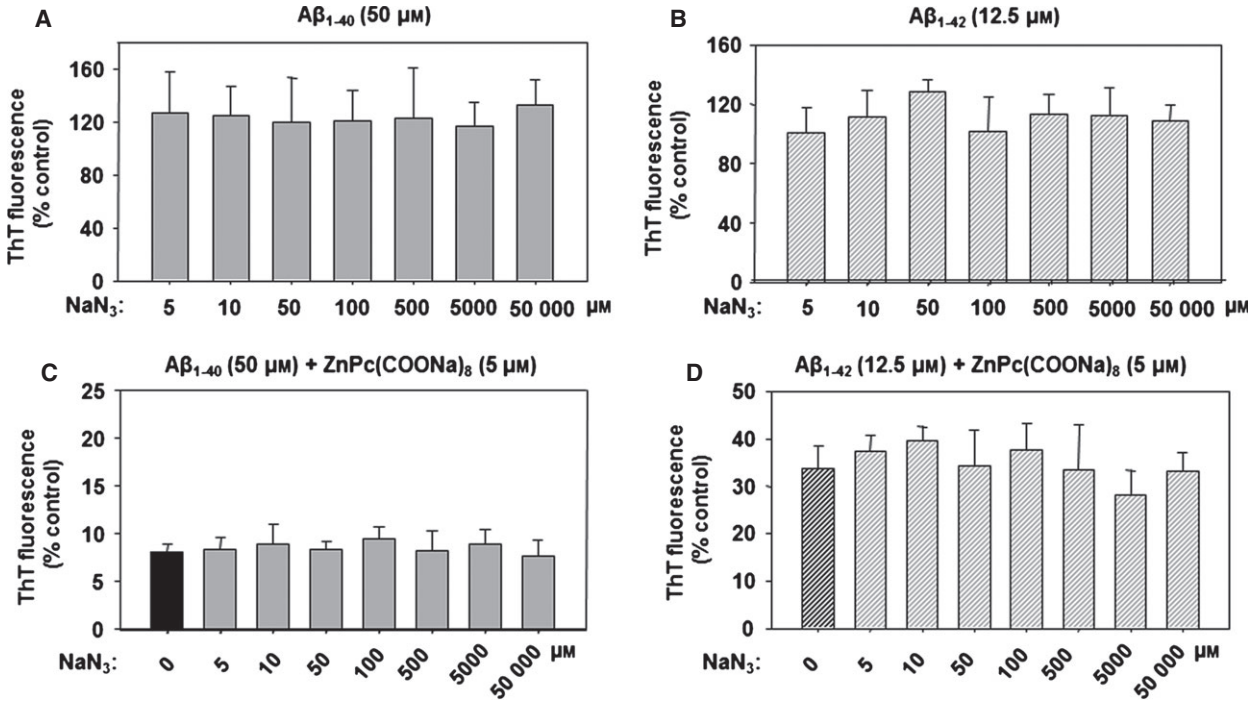

Fig. 5. Effect of sodium azide (NaN_3) on $ZnPc(COONa)_8$-mediated inhibition of Aβ fibril formation. (A,B) The indicated concentration of NaN_3 was added to $A\beta_{1\text{-}40}$ (50 μM) (A) or $A\beta_{1\text{-}42}$ (12.5 μM) (B), and the mixtures were incubated for 48 and 24 h, respectively. (C,D) To evaluate the effects of NaN_3 on $ZnPc(COONa)_8$-mediated inhibition of $A\beta_{1\text{-}40}$ and $A\beta_{1\text{-}42}$ fibril formation, the indicated concentrations of NaN_3 were added to $A\beta_{1\text{-}40}$ (50 μM) (C) and $A\beta_{1\text{-}42}$ (12.5 μM) (D) in the presence of $ZnPc(COONa)_8$ (5 μM), and the mixtures were incubated for 48 and 24 h, respectively. The amount of fibrils formed after incubation was evaluated by a ThT fluorescence assay. Values are means ± SEM of at least three experiments, and are presented as a percentage of the control condition (Aβ peptide alone).

[18], and that iron-containing phthalocyanine promotes conversion of $A\beta_{1\text{-}40}$ oligomer to a fibril meshwork [19]. In the present work, the two carboxylated phthalocyanines were water-soluble, while ZnPc $(COOC_5H_{11})_8$ and the PdPc dimer were not, and, as only the carboxylated phthalocyanines inhibited Aβ fibril formation, the differential interaction with Aβ may reflect the differences in hydrophilicity of the compounds. Interestingly, $ZnPc(COONa)_8$ showed a much stronger inhibitory effect than $ZnPc(COONa)_{16}$ despite having similar solubility, so structural differences also appear to be important. In addition, ZnPc $(COONa)_8$ had a much greater inhibitory effect on $A\beta_{1\text{-}40}$ than on $A\beta_{1\text{-}42}$ fibril formation. Fibril formation for both $A\beta_{1\text{-}40}$ and $A\beta_{1\text{-}42}$ is a nucleation-dependent process, in which the surfactant properties of the peptide, provided by the hydrophobic amino acids at the C-terminus, play a pivotal role [31]. $A\beta_{1\text{-}42}$ polymerizes much faster than $A\beta_{1\text{-}40}$ because of the presence of two more hydrophobic amino acids at the C-terminus [32], and this may also account at least in part for the differential interaction of $ZnPc(COONa)_8$ with the peptides.

$ZnPc(COONa)_8$ not only inhibited the Aβ fibril formation process, but also destabilized pre-formed fibrils. Fibril formation is a dynamic process, in which association of monomers to form polymers, and dissociation of the polymers to monomers and other low-molecular-weight species, occur side by side. Initially, the concentrations of monomer and other low-molecular-weight species are high. As a result, the rate of association is greater than that of dissociation, while, at the plateau stage, the rates of association and dissociation are in equilibrium [33]. Our binding assay showed that $ZnPc(COONa)_8$ had a higher binding ability to monomers and other low-molecular-weight species than to pre-formed Aβ fibrils. In the destabilization experiment, monomers and low-molecular-weight species of Aβ may preferentially bind to ZnPc $(COONa)_8$ after dissociation from the fibrils, disturbing the fibril formation equilibrium. We confirmed that addition of $ZnPc(COONa)_8$ to fibrils increases the amount of low-molecular-weight species, at least in the case of $A\beta_{1\text{-}40}$.

Pthalocyanines are known to produce singlet oxygen in the presence of light [23], and singlet oxygen inter-

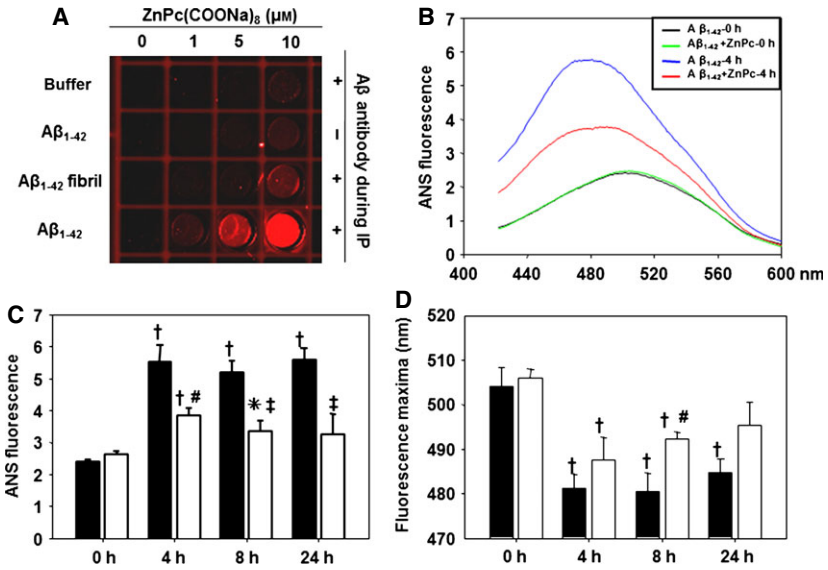

Fig. 6. Binding of $ZnPc(COONa)_8$ to $A\beta_{1-42}$ and change in the hydrophobicity of the fibril-forming microenvironment. (A) To evaluate the binding ability to pre-formed fibrils, $A\beta_{1-42}$ fibrils were prepared by incubating $A\beta_{1-42}$ monomer (50 μM) in fibril-forming buffer for 24 h, then the indicated concentration of $ZnPc(COONa)_8$ was added to the fibrils to give a final concentration of 50 μM, and incubation was continued for 24 h. After incubation, 5 μg of peptide fibrils was used for immunoprecipitation with a monoclonal anti-Aβ IgG. For negative controls, normal mouse IgG was used instead of anti-Aβ IgG, or buffer containing only $ZnPc(COONa)_8$ was used (without $A\beta_{1-42}$). (B–D) To evaluate the hydrophobic microenvironment, $A\beta_{1-42}$ (12.5 μM) was incubated in the absence or presence of $ZnPc(COONa)_8$ (5 μM) for the indicated times, and an ANS fluorescence assay was performed as described in Experimental procedures. (B) Representative ANS fluorescence emission spectra of $A\beta_{1-42}$ in the absence or presence of $ZnPc(COONa)_8$ at indicated times. (C,D) Mean values of ANS fluorescence intensities (arbitrary units) and the positions of fluorescence emission maxima (nm). Symbols indicate statistically significant differences compared with the corresponding 0 h condition ($^{*}P < 0.05$, $^{\dagger}P < 0.01$), or compared with the $A\beta_{1-42}$ experiment at the same time point ($^{\#}P < 0.05$, $^{\ddagger}P < 0.01$).

acts with various biomolecules, including proteins. Therefore, we investigated whether singlet oxygen has a role in the inhibition of fibril formation. However, sodium azide, a scavenger of singlet oxygen [24], did not influence the inhibitory effect of $ZnPc(COONa)_8$, suggesting that singlet oxygen plays no role in the process.

We found that ZnPc binds to Aβ peptides during fibril formation, and this binding may play a role in the inhibition of fibril formation. Compounds with an aromatic ring structure may interact with amyloid-forming peptides [34,35], but non-inhibitory phthalocyanines such as $ZnPc(COOC_5H_{11})_8$ also contain aromatic rings. As the inhibitory effect was specific to $ZnPc(COONa)_8$ and $ZnPc(COONa)_{16}$, other parts of the compound besides the aromatic rings, such as the sodium carboxylated side chains, may be more important for the interaction. Zinc ions interact with Aβ peptides and modulate fibril formation [36,37], but the differential effects of $ZnPc(COONa)_8$ and $ZnPc(COONa)_{16}$ on Aβ fibril formation suggest that this is not a major factor. We consider that the presence of sodium carboxylate groups, as well as their number in ZnPc are important for the interaction with Aβ peptide.

The nucleation-dependent Aβ aggregation process involves hydrophobic interaction of the C-terminal hydrophobic amino acids in an aqueous environment [29,30]. ANS, a hydrophobic fluorescent dye, is widely used to probe protein conformational changes, as its fluorescence dramatically increases in a hydrophobic environment [28]. We found that addition of $ZnPc(COONa)_8$ caused an early and sustained reduction of ANS fluorescence. As different molecular species, such as oligomers, pre-fibrillar aggregates and mature fibrils, may have different binding affinity to ANS, the change in the ANS fluorescence may reflect changes in the proportions of the various molecular species of Aβ caused by binding of $ZnPc(COONa)_8$. The β-sheet structures of Aβ, which is affected by the hydrophobic environment [25], was decreased by $ZnPc(COONa)_8$ from an early time point during fibril formation. We found that Aβ monomers, dimers, trimers and tetramers decreased over time, while larger oligomers increased during fibril formation. However, in the presence of $ZnPc(COONa)_8$, the reduction of low-

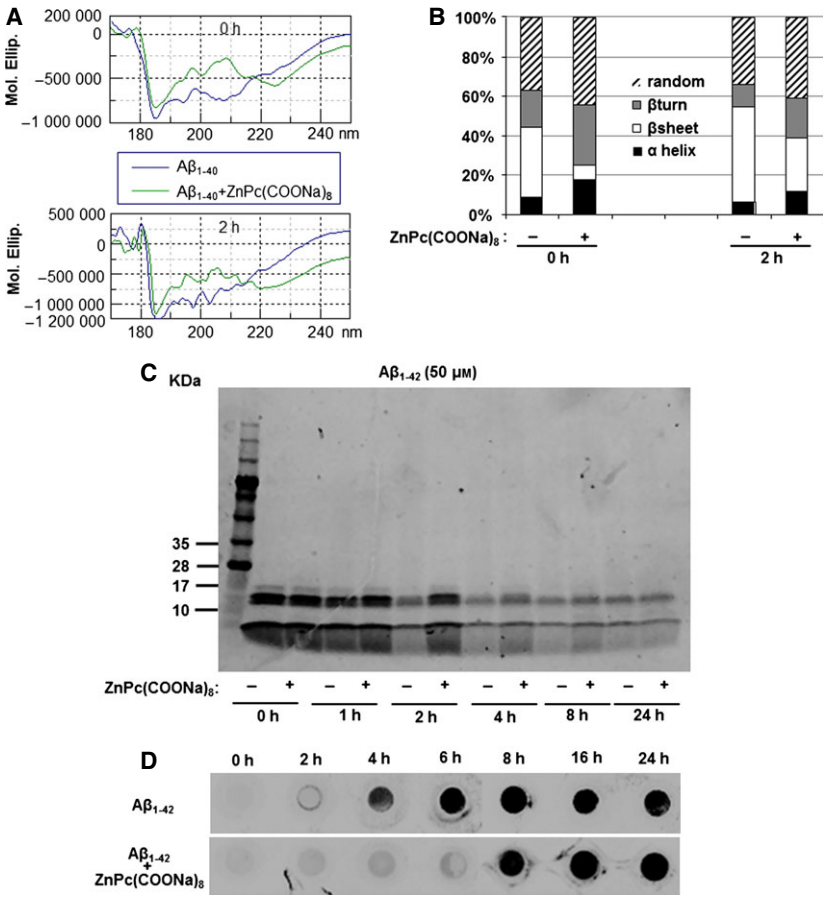

Fig. 7. Effects of $ZnPc(COONa)_8$ on secondary structure and oligomerization of the Aβ peptide. $Aβ_{1-40}$ (100 μM) was incubated in fibril-forming buffer in the absence or presence of $ZnPc(COONa)_8$ (2 μM) for the indicated times. The samples were then diluted with H_2O to give $Aβ_{1-40}$ and $ZnPc(COONa)_8$ concentrations of 10 and 0.2 μM, respectively, and the changes in secondary structure were evaluated by CD spectroscopy. (A) Representative CD spectra of $Aβ_{1-40}$ alone or $Aβ_{1-40}$ with $ZnPc(COONa)_8$ incubated for 0 and 2 h. (B) Percentage of different secondary structures in a representative experiment. (C) $Aβ_{1-42}$ (50 μM) was incubated in fibril-forming buffer in the absence or presence of $ZnPc(COONa)_8$ (5 μM) for the indicated time. Two micrograms of peptide was separated by SDS/PAGE using a 4-20% gradient Tris-glycine gel, and peptide bands for $Aβ_{1-42}$ species were visualized by Coomassie Brilliant Blue staining, as described in Experimental procedures. (D) After incubation, 2 μg peptide was spotted on a nitrocellulose membrane, and $Aβ_{1-42}$ oligomers were detected using oligomer-specific antibody, as described in Experimental procedures.

molecular-weight species and the appearance of oligomers were delayed. Taken together, our results suggest that $ZnPc(COONa)_8$ alters the fibril formation microenvironment, thereby inhibiting nucleation and oligomerization.

Finally, we examined the effect of ZnPc on neuronal viability. In agreement with previous studies [38], our preliminary experiments showed that $ZnPc(COONa)_8$ accumulated inside the cells in a neuronal cell culture system (data not shown). Nevertheless, $ZnPc(COONa)_8$ alone did not decrease the cell viability; rather it provided at least some protection against Aβ-induced neurotoxicity. Aβ oligomers are considered to be the most toxic species of Aβ [11,12]. Thus, the decrease in oligomer formation by $ZnPc(COONa)_8$ may account for the neuroprotective effect.

In conclusion, our results indicate that water-soluble $ZnPc(COONa)_8$ binds to Aβ peptides and inhibits oligomerization and subsequent fibril formation processes. It also destabilizes pre-formed fibrils. We consider that $ZnPc(COONa)_8$ has potential value as a diagnostic probe for NIR imaging of fibrils in AD brains, and may also be a candidate for treatment of AD.

Experimental procedures

Materials

$Aβ_{1-40}$ and $Aβ_{1-42}$ were purchased from the Peptide Institute (Osaka, Japan). The peptides were dissolved in 0.1% NH_3 at a concentration of 250 μM, immediately divided into aliquots, and stored at −70°C. Chromatographic data provided by the manufacturer indicated monomeric form of the peptides. ThT and filter-sterilized deionized water were purchased from Wako Pure Chemicals (Richmond, VA) and Sigma-Aldrich (St Louis, MO), respectively. Prestained protein size markers were obtained from Nippon Genetics Europe (Duren, Germany), and 4–20% Tris-glycine polyacrylamide was obtained from Bio-Rad (Hercules, CA). Nitrocellulose membrane for the dot-blot assay was obtained from Millipore (Billerica, MA).

Synthesis of phthalocyanines

In this study, four phthalocyanines were used. $ZnPc(COONa)_8$ and $ZnPc(COONa)_{16}$ were dissolved in H_2O. $ZnPc(COOC_5H_{11})_8$ and PdPc dimer were dissolved in chloroform. The phthalocyanines were each dissolved at 1 mM concentration,

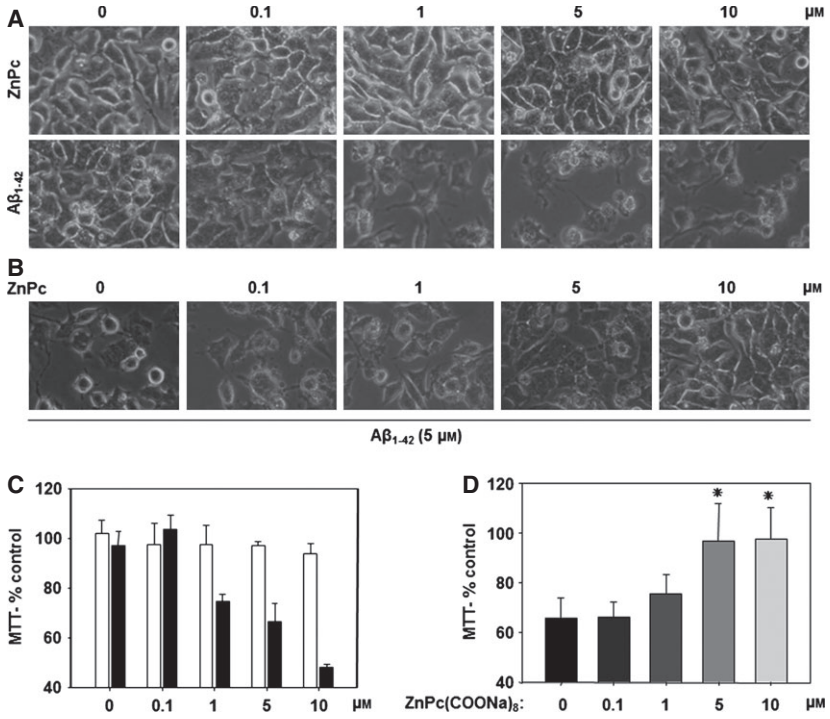

Fig. 8. Effects of $ZnPc(COONa)_8$ on neuronal viability in culture. (A) Cells of a neuronal cell line (A1) were cultured in Dulbecco's modified Eagle's medium containing 1% fetal bovine serum in the presence of the indicated concentrations of $ZnPc(COONa)_8$ or $A\beta_{1\text{-}42}$ for 48 h. Representative photomicrographs of A1 cells cultured with $ZnPc(COONa)_8$ (top row) or $A\beta_{1\text{-}42}$ (bottom row) are shown. (B) A1 cells were treated with $A\beta_{1\text{-}42}$ (5 μM) and the indicated concentrations of $ZnPc(COONa)_8$, and representative photomicrographs after 48 h treatment are shown. (C) After treatment with the indicated concentrations of $A\beta_{1\text{-}42}$ or $ZnPc(COONa)_8$ for 48 h, the viability of A1 cells were evaluated by the MTT assay. Values are means ± SEM for three experiments; white bars-$ZnPc(COONa)_8$; black bars-$A\beta_{1\text{-}42}$. (D) A1 cells were cultured with $A\beta_{1\text{-}42}$ (5 μM) and the indicated concentrations of $ZnPc(COONa)_8$ for 48 h, and cell viability was evaluated by the MTT assay, as described in Experimental procedures. The data presented in (C) and (D) are percentages of the control (viable cells in normal culture). Symbols indicate statistically significant differences compared with the 0 μM $ZnPc(COONa)_8$ condition (*$P < 0.05$).

and the solutions were stored at -20°C until use. Preparation of these phthalocyanines [39,40] is described below.

$ZnPc(COOC_5H_{11})_8$

A mixture of 4,5-dichlorophthalonitrile (1.0 g, 5.1 mmol) and *n*-hexyl-4-hydroxylbenzoate (4.3 g, 19.3 mmol) in dimethylformamide (60 mL) was stirred in the presence of K_2CO_3 (4 x 4 g) at 65°C for 24 h. The reaction mixture was poured into ice-cold water to give a whitish–brown precipitate, which was extracted with $CHCl_3$ (5 x 100 mL). The organic extracts were dried over anhydrous $MgSO_4$ (25 g), and concentrated under vacuum to give a yellow oil. Re-crystallization from methanol gave 4,5-bis[(4-hexyloxycarbonyl)phenoxy]phthalonitrile as a white solid (yield 2.2 g). The obtained compound (460 mg, 0.81 mmol) was used for reaction with $Zn(OAc)_2{\cdot}2\ H_2O$ (65 mg, 0.30 mmol) in *n*-pentanol (10 mL) containing a few drops of 1,8-diazabicyclo[5.4.0]undec-7-ene. The reaction mixture was refluxed overnight, and then volatiles were removed under reduced pressure to give a greenish blue solid. During the nitrile cyclization reaction in *n*-pentanol, hexyloxy groups on the nitrile were replaced with pentoxy groups from the reaction solvent. Re-crystallization of the crude product from $EtOH/H_2O$ gave the compound ZnPc $(COOC_5H_{11})_8$ as a green solid (yield 280 mg).

$ZnPc(COONa)_{16}$

A mixture of 4,5-dichlorophthalonitrile, 5-hydroxyisophthalate and K_2CO_3 in dimethylformamide was stirred at 65°C for 24 h, and then poured into ice-cold water to give a white–brown precipitate, which was extracted using $CHCl_3$. The organic extracts were dried over anhydrous $MgSO_4$, and concentrated under vacuum to give a yellow oil. Re-crystallization from methanol produced 4,5-bis[(3,5-bismethoxycarbonyl) phenoxy]phthalonitrile (1st compound) as a white solid.

The 1st compound was mixed with $Zn(OAc)_2{\cdot}2\ H_2O$ and a few drops of 1,8-diazabicyclo[5.4.0]undec-7-ene in *n*-pentanol, and refluxed overnight. The volatiles were removed under vacuum to give a greenish blue solid, which was purified by column chromatography using dichloromethane/ethyl acetate (20:1). The crude product was re-crystallized from tetrahydrofuran/MeOH to give the 2nd compound zinc (II)

2,3,9,10,16,17,23,24-octakis[(3′,5′-bispentyloxycarbonyl)phenoxy]phthalocyanine as a green solid.

The 2nd compound was dissolved in tetrahydrofuran, and the solution was added slowly to a saturated NaOH solution in water/methanol (1:5) (100 mL). The mixture was stirred at 40°C for 4 h. The resulting precipitate was collected by filtration, washed repeatedly with MeOH and $CHCl_3$ at room temperature, dissolved in water, and neutralized with 1 M HCl (to pH 7). The compound ZnPc $(COONa)_{16}$ was precipitated as a green solid upon addition of ethanol.

$ZnPc(COONa)_8$

A saturated NaOH solution in water/methanol (1:5) (100 mL) was added slowly to a tetrahydrofuran (5 mL) solution of $ZnPc(COOC_5H_{11})_8$ (200 mg). The mixture was stirred at 40°C for 4 h. The resulting precipitate was collected by filtration, washed repeatedly with MeOH and $CHCl_3$, dissolved in water, and neutralized with 1 M HCl (to pH 7). Ethanol was added to precipitate ZnPc $(COONa)_8$ as a green solid (yield 66 mg).

PdPc dimer

A mixture of 4,5-bis(2,6-dimethylphenoxy)phthalonitrile (997 mg, 2.7 mmol), bis(1,3-diiminoisoindoline) (115 mg, 0.54 mmol) and $PdCl_2$ (295 mg, 1.7 mmol) in *n*-propanol (10 mL) and 1,8-diazabicyclo[5.4.0]undec-7-ene (1.0 mL) was heated at 110°C for 30 h. After the reaction mixture had cooled, toluene (30 mL) was added, and the resulting precipitate was collected by filtration, and vacuum-dried to give a green solid. This product was dissolved in toluene and subjected to gel filtration chromatography with toluene as an eluent to produce two major fractions. PdPc dimer was obtained from the first fraction (yield 112 mg) and PcPc was obtained from the second fraction (yield 645 mg).

Aβ fibril formation

Synthetic Aβ peptides were added to fibril-forming buffer (50 mM phosphate buffer, pH 7.5, 100 mM NaCl) containing various concentrations of phthalocyanines [41]. As a control, peptides were added to fibril-forming buffer without phthalocyanines (addition of solvent only). The reaction mixtures were incubated for indicated times at 37°C without agitation, and then the reaction was terminated by freezing the samples quickly.

Quantification of Aβ fibril formation

Aβ fibril formation was determined by ThT fluorescence spectroscopy [41]. Samples were diluted tenfold with glycine (pH 8.5, 50 mM final concentration), then ThT was added (5 μM final concentration), and the fluorescence signal was measured with excitation at 446 nm and emission at 490 nm using an F2500 spectrofluorimeter (Hitachi, Tokyo, Japan). The florescence intensity of Aβ fibrils in a sample was normalized by subtracting the fluorescence intensity of the buffer alone.

For further evaluation of fibril formation, 25 μg $Aβ_{1-42}$ at 100 μM concentration in the absence or presence of $ZnPc(COONa)_8$ (5 μM) was used for fibril formation for 24 h. The fibrils were removed from the samples using an Amicon 100 kDa cut-off filter (Millipore), and the filtrates were concentrated by evaporation. Total protein in the filtrates was measured using an ND-1000 UV/Vis spectrophotometer (NanoDrop Technologies, Wilmington, DE) by evaluating absorbance at 280 nm.

Electron microscopic analysis of Aβ fibrils

Electron microscopic analysis of Aβ fibrils was performed as described previously [41]. Briefly, after incubation of Aβ (50 μM) in the absence or presence of $ZnPc(COONa)_8$ (5 μM) for the desired times, a 5 μL sample was applied to a carbon-coated Formvar grid (Nisshin EM Co., Tokyo, Japan). After incubation for 1 min, an equal volume of 0.5% v/v glutaraldehyde solution was applied to displace the sample, and incubation was continued for an additional 1 min. The grid was washed with water and dried. Then 10 μL of 2% w/v uranyl acetate solution was applied, and the grid was incubated for 2 min. Finally, excess uranyl acetate was soaked with a paper towel, and the grid was air-dried and examined under an EM-002B electron microscope (Topcon, Tokyo, Japan).

ANS fluorescence assay

To analyze the relative exposure of hydrophobic surfaces of $Aβ_{1-42}$, we measured the change in the fluorescence intensity of ANS (Sigma-Aldrich), using a Hitachi F2500 spectrofluorimeter. The excitation wavelength was 360 nm, and emission was scanned from 380–600 nm at a rate of 300 nm·min^{-1}. The slit widths for excitation and emission were 5 nm. Maximum emission values are means ± SEM of three independent experiments, and are expressed in arbitrary fluorescence units.

Gel electrophoresis analysis of Aβ

After fibril formation, Aβ samples were separated by SDS/PAGE using a 4–20% gradient Tris-glycine gel (Bio-Rad). For electrophoresis, 2 x SDS non-reducing sample buffer (Invitrogen, Carlsbad, CA) was added to 2 μg Aβ peptide in a final volume of 20 μL, and the mixture was incubated for 2 min at 85°C. After electrophoresis, the gel was fixed using fixation buffer (40% methanol, 10% acetic acid) for

30 min, and then stained for 1 h using Biosafe Coomassie Brilliant Blue G250 (Bio-Rad). After staining, the gel was washed overnight with water, and scanned using a gel scanner (Bio-Rad).

Determination of oligomers by dot-blot immunoassay

After fibril formation, aliquots equivalent to 2 μg $A\beta_{1\text{-}42}$ peptide were spotted on a nitrocellulose membrane. To detect oligomer, an oligomer-specific antibody (A11, Invitrogen) was used; this antibody specifically reacts with a variety of soluble oligomeric protein/peptide aggregates including Aβ, regardless of their amino acid sequence, and does not react with monomer species or insoluble fibrils of protein/peptide [42]. In the case of Aβ oligomer, it has been shown to react with species of at least octamer in size. To detect immunoreactive oligomers, an infrared dye conjugated anti-rabbit IgG and Odyssey infrared dye scanning system (Li-Cor Biosciences, Lincoln, NE) were used according to the manufacturer's instructions.

Phthalocyanine binding assay

To evaluate the binding of $ZnPc(COONa)_8$ to $A\beta_{1\text{-}42}$ peptide, Aβ fibrils were prepared by incubation of the peptide in fibril-forming buffer for 24 h, then indicated concentrations of $ZnPc(COONa)_8$ were added to the fibril equivalent to a peptide concentration of 50 μM, and incubation was continued for 24 h. A sample containing 5 μg peptide was immunoprecipitated with a monoclonal Aβ-specific antibody (Santa Cruz, Dallas, TX). The immunoprecipitates were taken in a ELISA plate and scanned at 680 nm using an Odyssey infrared scanner (Li-Cor) to detect $ZnPc(COONa)_8$. Two negative controls were run, comprising fibril-forming buffer alone containing the indicated concentrations of $ZnPc(COONa)_8$ immunoprecipitated with Aβ-specific antibody, and use of mouse normal IgG for immunoprecipitation instead of Aβ-specific antibody.

Analysis of secondary structures of Aβ peptide

To prepare samples for evaluation of changes of secondary structures during fibril formation, $ZnPc(COONa)_8$ (2 μM) was added to $A\beta_{1\text{-}40}$ monomers (100 μM) in fibril-forming buffer, and the mixture was incubated at 37°C for 0 and 2 h. The samples were diluted with water to obtain final concentrations of $A\beta_{1\text{-}40}$ and $ZnPc(COONa)_8$ of 10 and 0.2 μM, respectively. Then CD spectra in the range 190–250 nm were acquired at 50 $nm \cdot min^{-1}$ using a Jasco J-720 spectropolarimeter (Jasco Corporation, Tokyo, Japan) and a quartz cell with 3 mm optical path length. The results are expressed as mean of residue molar ellipticity of 5 scans, and the percentages of secondary structures in the samples were estimated using the Protein Secondary Structure Estimation Program (Jasco Corp.) using published reference CD spectra [43].

Cell culture

Human neuronal cell line A1 was generated by somatic fusion between a human fetal cerebral neuron and a human neuroblastoma cell, and shows characteristic morphological, electrophysiological and expressional features of neurons [44]. A1 cells were cultured in Dulbecco's modified Eagle's medium (Wako Pure Chemicals) containing 5% fetal bovine serum (Gibco, Invitrogen). During stimulation with $A\beta_{1\text{-}42}$ and $ZnPc(COONa)_8$, the concentration of fetal bovine serum was reduced to 1%. Photomicrographs of the cultured cells were obtained using an inverted cell culture microscope (Olympus CK-2, Olympus, Tokyo, Japan) equipped with a digital photography system (Olympus).

MTT cell viability assay

The effect of $ZnPc(COONa)_8$ on Aβ-induced neuronal toxicity was evaluated by an MTT cell viability assay, as described previously [45]. Briefly, A1 cells (3×10^3/well) were seeded into wells of a 96-well plate and cultured for 48 h. The cells were treated with the indicated concentrations of $ZnPc(COONa)_8$, $A\beta_{1\text{-}42}$ or both $A\beta_{1\text{-}42}$ and $ZnPc(COONa)_8$ in 100 μL Dulbecco's modified Eagle's medium containing 1% fetal bovine serum for 48 h. After incubation, 20 μL of MTT solution (Sigma-Aldrich) (5 $mg \cdot mL^{-1}$) was added to the culture medium, and incubation was continued for 3.5 h at 37°C. Then the medium was removed carefully, MTT solvent (4 mM HCl, 0.1% Nonidet® P-40 (Nacalai Tesque, Kyoto, Japan) in isopropanol) was added, and incubation was continued for 15 min at room temperature with protection from light. The absorbance was read at 590 nm. The absorbance of the cells under normal culture conditions was used as a control.

Statistical analysis

The results are expressed as means ± SEM of at least three independent experiments. Statistical analysis to compare mean values was performed using one-way ANOVA, followed by Scheffe's post hoc test, or Student's *t* test. Fibril formation kinetics were analyzed using SigmaPlot software (Systat Software Inc, San Jose, CA, USA), and *P* values < 0.05 were taken as indicating statistical significance.

Acknowledgements

This study was supported by Japan Society for the Promotion of Science KAKENHI grant number 24310102.

Author contributions

ST planned and performed the experiments, analyzed the data and prepared the manuscript. AS planned the experiments, analyzed the data and prepared the manuscript. SY analyzed the data and prepared the manuscript. MH prepared phthalocyanines, analyzed the data and prepared the manuscript. TI prepared phthalocyanines, analyzed the data and prepared the manuscript. AN planned the experiments, provided the reagents and other essential materials, prepared the manuscript, and supervised the overall study.

References

1 Rowland LP, Pedley TA & Merritt HH (2010) Merritt's Neurology, 12 edn. pp. 713–717. Lippincott Williams & Wilkins, Philadelphia, PA.

2 Duyckaerts C, Delatour B & Potier MC (2009) Classification and basic pathology of Alzheimer disease. *Acta Neuropathol* **118**, 5–36.

3 Francis PT, Palmer AM, Snape M & Wilcock GK (1999) The cholinergic hypothesis of Alzheimer's disease: a review of progress. *J Neurol Neurosurg Psychiatry* **66**, 137–147.

4 Campion D, Flaman JM, Brice A, Hannequin D, Dubois B, Martin C, Moreau V, Charbonnier F, Didierjean O, Tardieu S *et al.* (1995) Mutations of the presenilin I gene in families with early-onset Alzheimer's disease. *Hum Mol Genet* **4**, 2373–2377.

5 Goate A, Chartier-Harlin MC, Mullan M, Brown J, Crawford F, Fidani L, Giuffra L, Haynes A, Irving N, James L *et al.* (1991) Segregation of a missense mutation in the amyloid precursor protein gene with familial Alzheimer's disease. *Nature* **349**, 704–706.

6 Hardy J & Selkoe DJ (2002) The amyloid hypothesis of Alzheimer's disease: progress and problems on the road to therapeutics. *Science* **297**, 353–356.

7 Richards SJ, Waters JJ, Beyreuther K, Masters CL, Wischik CM, Sparkman DR, White CL 3rd, Abraham CR & Dunnett SB (1991) Transplants of mouse trisomy 16 hippocampus provide a model of Alzheimer's disease neuropathology. *EMBO J* **10**, 297–303.

8 Sisodia SS, Kim SH & Thinakaran G (1999) Function and dysfunction of the presenilins. *Am J Hum Genet* **65**, 7–12.

9 Xia W, Zhang J, Kholodenko D, Citron M, Podlisny MB, Teplow DB, Haass C, Seubert P, Koo EH & Selkoe DJ (1997) Enhanced production and oligomerization of the 42-residue amyloid beta-protein by Chinese hamster ovary cells stably expressing mutant presenilins. *J Biol Chem* **272**, 7977–7982.

10 Yoshioka K, Miki T, Katsuya T, Ogihara T & Sakaki Y (1991) The 717Val—Ile substitution in amyloid precursor protein is associated with familial Alzheimer's disease regardless of ethnic groups. *Biochem Biophys Res Commun* **178**, 1141–1146.

11 Cotman CW, Whittemore ER, Watt JA, Anderson AJ & Loo DT (1994) Possible role of apoptosis in Alzheimer's disease. *Ann N Y Acad Sci* **747**, 36–49.

12 Malaplate-Armand C, Florent-Béchard S, Youssef I, Koziel V, Sponne I, Kriem B, Leininger-Muller B, Olivier JL, Oster T & Pillot T (2006) Soluble oligomers of amyloid-beta peptide induce neuronal apoptosis by activating a cPLA2-dependent sphingomyelinase-ceramide pathway. *Neurobiol Dis* **23**, 178–189.

13 Iqbal K, Liu F & Gong CX (2014) Alzheimer disease therapeutics: focus on the disease and not just plaques and tangles. *Biochem Pharmacol* **88**, 631–639.

14 Leger GC & Massoud F (2013) Novel disease-modifying therapeutics for the treatment of Alzheimer's disease. *Expert Rev Clin Pharmacol* **6**, 423–442.

15 Cruchaga C, Ebbert MT & Kauwe JS (2014) Genetic discoveries in AD using CSF amyloid and tau. *Curr Genet Med Rep* **2**, 23–29.

16 Petrella JR (2013) Neuroimaging and the search for a cure for Alzheimer disease. *Radiology* **269**, 671–691.

17 Hilderbrand SA & Weissleder R (2010) Near-infrared fluorescence: application to in vivo molecular imaging. *Curr Opin Chem Biol* **14**, 71–79.

18 Lee EN, Cho HJ, Lee CH, Lee D, Chung KC & Paik SR (2004) Phthalocyanine tetrasulfonates affect the amyloid formation and cytotoxicity of alpha-synuclein. *Biochemistry* **43**, 3704–3715.

19 Park JW, Ahn JS, Lee JH, Bhak G, Jung S & Paik SR (2008) Amyloid fibrillar meshwork formation of iron-induced oligomeric species of Abeta40 with phthalocyanine tetrasulfonate and its toxic consequences. *ChemBioChem* **9**, 2602–2605.

20 Simon J & Vacus J (1995) Luminescence and anti-aggregative properties of polyoxyethylene-substituted phthalocyanine complexes. *Adv Mater* **7**, 797–800.

21 Spikes JD (1986) Phthalocyanines as photosensitizers in biological systems and for the photodynamic therapy of tumors. *Photochem Photobiol* **43**, 691–699.

22 Moss MA, Varvel NH, Nichols MR, Reed DK & Rosenberry TL (2004) Nordihydroguaiaretic acid does not disaggregate beta-amyloid(1-40) protofibrils but does inhibit growth arising from direct protofibril association. *Mol Pharmacol* **66**, 592–600.

23 Agarwal R, Athar M, Urban SA, Bickers DR & Mukhtar H (1991) Involvement of singlet oxygen in chloroaluminum phthalocyanine tetrasulfonate-mediated photoenhancement of lipid peroxidation in rat epidermal microsomes. *Cancer Lett* **56**, 125–129.

24 Bancirova M (2011) Sodium azide as a specific quencher of singlet oxygen during chemiluminescent detection by luminol and Cypridina luciferin analogues. *Luminescence* **26**, 685–688.

25 Kowalewski T & Holtzman DM (1999) In situ atomic force microscopy study of Alzheimer's beta-amyloid peptide on different substrates: new insights into mechanism of beta-sheet formation. *Proc Natl Acad Sci USA* **96**, 3688–3693.
26 Marshall KE, Morris KL, Charlton D, O'Reilly N, Lewis L, Walden H & Serpell LC (2011) Hydrophobic, aromatic, and electrostatic interactions play a central role in amyloid fibril formation and stability. *Biochemistry* **50**, 2061–2071.
27 Tjernberg LO, Callaway DJ, Tjernberg A, Hahne S, Lilliehöök C, Terenius L, Thyberg J & Nordstedt C (1999) A molecular model of Alzheimer amyloid beta-peptide fibril formation. *J Biol Chem* **274**, 12619–12625.
28 Hawe A, Sutter M & Jiskoot W (2008) Extrinsic fluorescent dyes as tools for protein characterization. *Pharm Res* **25**, 1487–1499.
29 Hills RD Jr & Brooks CL 3rd (2007) Hydrophobic cooperativity as a mechanism for amyloid nucleation. *J Mol Biol* **368**, 894–901.
30 Serpell LC (2000) Alzheimer's amyloid fibrils: structure and assembly. *Biochim Biophys Acta* **1502**, 16–30.
31 Soreghan B, Kosmoski J & Glabe C (1994) Surfactant properties of Alzheimer's A beta peptides and the mechanism of amyloid aggregation. *J Biol Chem* **269**, 28551–28554.
32 El-Agnaf OM, Mahil DS, Patel BP & Austen BM (2000) Oligomerization and toxicity of beta-amyloid-42 implicated in Alzheimer's disease. *Biochem Biophys Res Commun* **273**, 1003–1007.
33 Morris AM, Watzky MA & Finke RG (2009) Protein aggregation kinetics, mechanism, and curve-fitting: a review of the literature. *Biochim Biophys Acta* **1794**, 375–397.
34 Porat Y, Abramowitz A & Gazit E (2006) Inhibition of amyloid fibril formation by polyphenols: structural similarity and aromatic interactions as a common inhibition mechanism. *Chem Biology Drug Des* **67**, 27–37.
35 McLaughlin RW, De Stigter JK, Sikkink LA, Baden EM & Ramirez-Alvarado M (2006) The effects of sodium sulfate, glycosaminoglycans, and Congo red on the structure, stability, and amyloid formation of an immunoglobulin light-chain protein. *Protein Sci* **15**, 1710–1722.
36 Bush AI, Pettingell WH, Multhaup G, d Paradis M, Vonsattel JP, Gusella JF, Beyreuther K, Masters CL & Tanzi RE (1994) Rapid induction of Alzheimer A beta amyloid formation by zinc. *Science* **265**, 1464–1467.
37 Esler WP, Stimson ER, Jennings JM, Ghilardi JR, Mantyh PW & Maggio JE (1996) Zinc-induced aggregation of human and rat beta-amyloid peptides in vitro. *J Neurochem* **66**, 723–732.
38 Trivedi NS, Wang HW, Nieminen AL, Oleinick NL & Izatt JA (2000) Quantitative analysis of Pc 4 localization in mouse lymphoma (LY-R) cells via double-label confocal fluorescence microscopy. *Photochem Photobiol* **71**, 634–639.
39 Ikeue T, Sonoda M, Kurahashi S, Tachibana H, Teraoka D, Sugimori T, Kasuga K & Handa M (2010) Annulated dinuclear palladium (II) phthalocyanine complex as an effective photo-oxidation catalyst for near-infrared region light. *Inorganic Chemistry Comm* **13**, 1170–1172.
40 Liu W, Jensen TJ, Fronczek FR, Hammer RP, Smith KM & Vicente MG (2005) Synthesis and cellular studies of nonaggregated water-soluble phthalocyanines. *J Med Chem* **48**, 1033–1041.
41 Sheikh AM & Nagai A (2011) Lysophosphatidylcholine modulates fibril formation of amyloid beta peptide. *FEBS J* **278**, 634–642.
42 Kayed R, Head E, Thompson JL, McIntire TM, Milton SC, Cotman CW & Glabe CG (2003) Common structure of soluble amyloid oligomers implies common mechanism of pathogenesis. *Science* **300**, 486–489.
43 Yang JT, Wu CS & Martinez HM (1986) Calculation of protein conformation from circular dichroism. *Methods Enzymol* **130**, 208–269.
44 Nagai A, Suzuki Y, Baek SY, Lee KS, Lee MC, McLarnon JG & Kim SU (2002) Generation and characterization of human hybrid neurons produced between embryonic CNS neurons and neuroblastoma cells. *Neurobiol Dis* **11**, 184–198.
45 Nagai A, Ryu JK, Terashima M, Tanigawa Y, Wakabayashi K, McLarnon JG, Kobayashi S, Masuda J & Kim SU (2005) Neuronal cell death induced by cystatin C in vivo and in cultured human CNS neurons is inhibited with cathepsin B. *Brain Res* **1066**, 120–128.